

## **Evaluation of In-situ Variation of Water Content and Temperature Due to Soil-atmosphere Interaction by a Lysimeter Test**

by

Jidong TENG\* and Noriyuki YASUFUKU\*\*

(Received July 7, 2014)

### **Abstract**

Evaluation of the variation of water content and temperature due to soil-atmosphere interaction is very important for geotechnical and agricultural applications. An in-situ test was instrumented on basis of the developed lysimeter apparatus. The monitoring indexes in this test are volumetric water content, soil temperature, total weight of specimen, water percolation and the meteorological variables. The objective is to investigate the influence of climate changes on the soil response such as changes in water content and temperature. A numerical model based on HYDRUS-1D is also set up to analyze the interaction. Result shows that climate effects are limited to a shallow depth, which is 35 cm in this study. Moreover, comparisons between the measurements and simulations indicates the relevance of the adopted numerical approach.

**Keywords:** Lysimeter test, Evaporation, Infiltration, Water content profile, Soil temperature, HYDRUS-1D, Soil-atmosphere interaction

### **1. Introduction**

The simultaneous movements of liquid water, water vapor, and heat in the vadose zone plays a critical role in the overall water and energy balance of the near-surface environment of arid or semiarid region in many agriculture and engineering applications<sup>1)</sup>. The examples include evaluating the performance of engineered surface covers<sup>2-3)</sup>, soil salinization in arid and semi-arid region<sup>4)</sup>, geotechnical greening system for preventing desertification<sup>5)</sup> and so on. The soil-atmosphere interface is an important boundary condition affecting subsurface movement of liquid water, water vapor, and heat under field condition<sup>6)</sup>. Therefore, it is important to gain knowledge in the variation of water content and temperature due to local climate change.

The theoretical basis of soil-atmosphere interaction modelling has been development by many researchers, where the physical process of ground water flow and corresponding behavior of unsaturated soil can be numerically simulated when the climate, soil profile, and properties of a site are known<sup>1,6)</sup>. The variation of water content and soil temperature can be predicted based on these models. However, little field investigation on soil-atmosphere has been reported to real the

---

\* Post-Doctoral Fellow, Department of Civil Engineering

\*\* Professor, Department of Civil Engineering

mechanism and to verify the numerical schemes. Even if some researchers monitored the water content and temperature together meteorological indexes in a field site<sup>6-7)</sup>, the actual evaporation rate from soil surface is unclear, which is a really crucial parameter for soil-atmosphere interaction. In present work, a newly developed lysimeter test was introduced, which allows for timely measuring the actual evaporation rate and the profiles of water content and soil temperature. On one hand, the recorded data offer a better understanding of the soil-atmosphere interaction mechanism, on the other hand, they are quite valuable for the validation of numerical model dealing with in-situ water transfer. In addition, a coupled model for description of water (vapor and liquid) and heat transfers in soil is then performed using HRDRUS-1D. The model validated by measured result demonstrates how standard meteorological variables can be used for simulating diurnal changes in soil properties.

## 2. Description of lysimeter test

### 2.1 Design and instrument

The general concept of a weighing lysimeter requires four major elements. These include the container to hold the soil, water and vegetation; a rigid foundation; the force measuring or weighing system; and the data acquisition and analysis system<sup>8)</sup>. Accessory instrumentation is also required to measure and record climatic data. The design criteria for the lysimeter developed in this study are that (1) easily and rapidly deployed; (2) economical to construct and install; and (3) able to continuously monitor the change of water amount at the resolution of an hour. To meet these requirements as well as those of lysimeters in general, a number of constraints must be optimized. A field lysimeter facility was developed by geotechnical engineering laboratory aiming to obtain high sensitivity and precision combined with a low construction cost and simplicity of installation. The studied area was located at Ito campus of Kyushu University, Nishi-ku, Fukuoka-shi, Japan (33.3°N, 130.2°E). This site is an in-situ test area of Kyushu University. This location will facilitate providing the necessary management to insure continuous and reliable operation.

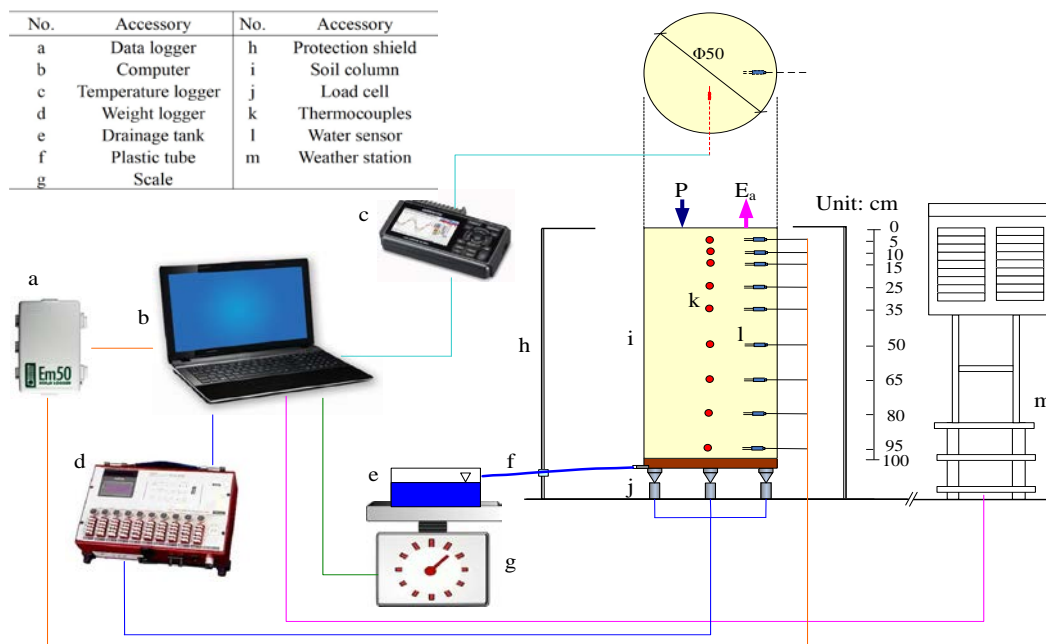
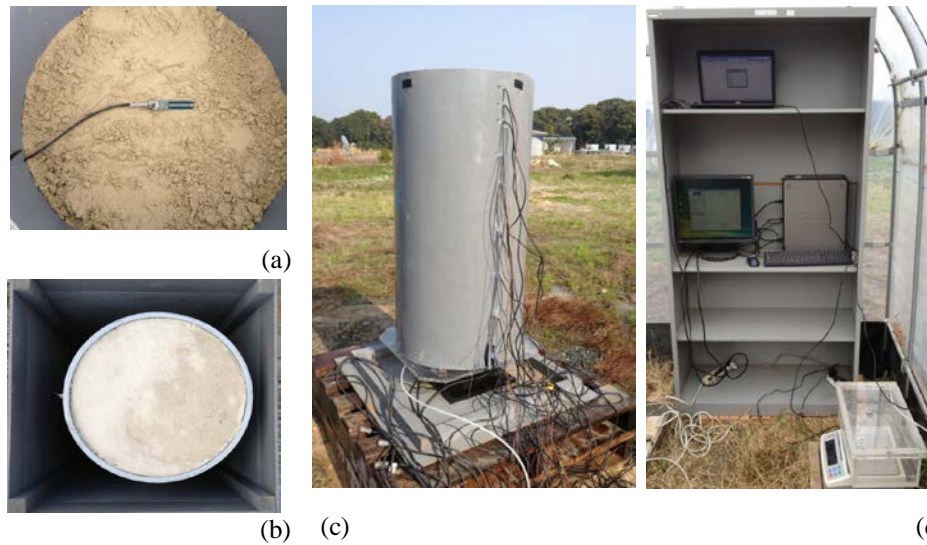


Fig. 1 Schematic illustration of lysimeter tests.



**Fig. 2** Photos of the in-situ test, (a) thermocouple and water moisture probe, (b) bird view of lysimeter, (c) soil column, (d) data acquisition system and percolation measuring system.

A layout of the instrumentation is presented in **Fig. 1**, the photo graphics of the equipment are presented in **Fig. 2**. A Cylindrical undisturbed lysimeters was performed, whose soil container is made of PVC material (105 cm in height, 50 cm in diameter, and 1.5 cm in wall thickness). At the bottom of cylinder, a 5 cm drainage layer was set and connected to a polyethylene tube allowing the water flow out. A steel plate was assembled at the bottom of lysimeter to support reinforce of system and to prevent the bottom plastic plate from bending. Three electronic load cells were equipped as equilateral triangle on the steel plate such that the lysimeter can stand stably. A plank protection shield was to insure the lysimeter from the influence of wind speed during weight measuring. The height of protection shield was 105 cm, the length and width were same at 60 cm. Nine thermocouples and nine water moisture probes were inserted to the cylinder to measure the instantaneous temperature and volumetric water content, respectively.

A cuboid Tank (20 cm in height, 20 cm in weight, and 40 cm in length) made of transparent acrylic material allowed for collecting all the water percolated. A polyethylene tube connected the tank to the bottom of the tank was used as drains. A scale (0.1g solution) gave a continuous weight measurement of both tank and collected water. The outputs of the load cells were recorded in a specific time interval by using a data logger, the load cells were connected directly to the data logger, and the output of each load cell was recorded separately in addition to the sum of the outputs of all three load cells. The thermocouples were connected to a midi Data Logger for the acquisition of temperature data. Two automatic ECH2O dielectric aquameters were connected with the soil moisture probe to collect the water content. Then all the data was accessed and stored by computers by specific data acquisition software. As for the accuracy of lysimeter, Payero and Irmak (2008)<sup>9</sup> indicated that lysimeter accuracy depended on the lysimeter area, mass, and the type of scale. In this study, the total solution of the load cells were 75 g that equaled to 0.38 mm of water change in soil specimen.

The weather data was available from Ito campus of Kyushu University and weather station in Itoshima city belonging to Japan meteorological Agency, which is about 3 km away from the in-situ test area. The weather station can provide the climatic parameters as rainfall; air temperature; air humidity; solar radiation; wind speed. Daily meteorological variables used in this

study are summarized in **Table 1**.

**Table 1** Weather variables recorded by the weather station.

Items	Reporting interval
Precipitation, mm	Daily total, hourly
Air temperature, °C	Daily average, daily max/min, hourly
Relative humidity, %	Daily max/min ,hourly
Solar radiation, kW/m <sup>2</sup>	Daily total, hourly
Wind speed, m/s	Daily average hourly

## 2.2 Experimental procedure

A solid foundation to support the mass of the lysimeter boxes was firstly constructed. Two leveled wooden frames (100 cm in length, 100 cm in width, and 15 cm in height) were constructed on top of the foundation. The surface of the wooden frames was set as even level. Then lysimeter was installed stably. Sampling or insulation of test material for the lysimeter was an important step in the lysimeter-leaching methodology. In this step, the characteristics of the test material could be altered by affecting either the physical properties as for example the macro pore structure by contaminating the sample. In this study, the K-7 sand was selected as the material due to its fine permeability and low swelling and shrinkage properties during wetting or drying. When packing the dry soil into the container, each time a layer of approximately 10 cm was added, and compaction energy was applied to the soil surface to achieve the maximum dry density of 1.50 g/cm<sup>3</sup>. At this time, the soil moisture probes and the thermocouples access tube were installed at different heights. When all the soil layers were in place, soil surface was made to be calm with reserving 2 cm from top edge of the container, which ensured the soil not being flowed out during test. After the fabrication of the lysimeter, water was supplied smoothly from the soil surface to saturate specimen. The infiltration process lasted about half hour until the water percolated from the drainage tube at the bottom of the container. Then water supply was stopped and the soil surface was covered by a plate. The drainage process continued about 3 days and then the initial condition was performed. The volumetric water contents of soil located at 5 cm, 10 cm, 15 cm, 25 cm, 35 cm, 50 cm, 65 cm, 80 cm, and 95 cm were 0.211, 0.176, 0.191, 0.186, 0.242, 0.261, 0.335, 0.407, and 0.414, respectively. At last, the protection shield was installed on the bottom plate, and all the probes were connected to corresponding data loggers.

Following installation of the lysimeter in the field, a calibration routine was followed to ensure the proper functioning and accuracy of the load cells. A series of known weights was placed one at a time on the lysimeter, and the total lysimeter weight was recorded. The weights were then removed one at a time with recording the total weight. The changes in weight recorded were then calculated and compared to the known changes in weight.

The lysimeter was installed in 23<sup>rd</sup>, March of 2013, and the test started from 27<sup>th</sup>, March to 15<sup>th</sup>, June of 2013, the duration was nearly 80 days. The measured data included: weights of lysimeter, weight of percolated water, instantaneous data of water content and soil temperature profile, weather indexes. All the data were registered electronically at 15 min intervals.

## 3. Numerical modelling

### 3.1 Models

The coupled movement of liquid water, water vapor, and heat in the subsurface, as well as interactions of these subsurface processes with the energy and water balances at the soil surface, is

implemented in the HYDRUS-1D code. The HYDRUS-1D is widely used, well-documented, and tested public domain code for simulating water and solute transport in soil<sup>11</sup>. Therefore, HYDRUS-1D is adopted as a countermeasure for numerical simulation to compare with the result of in-situ test.

The HYDRUS-1D program may be used to analyze water and solute movement in unsaturated, or fully saturated porous media<sup>11</sup>. The program numerically solves the Richards equation for saturated-unsaturated water flow and Fickian-based advection dispersion equations for heat and solute transport. The governing flow and transport equations are solved numerically using Galerkin type linear finite element schemes. Integration in time is achieved using an implicit (backwards) finite difference scheme for both saturated and unsaturated conditions. Additional measures are taken to improve solution efficiency for transient problems, including automatic time step adjustment and adherence to present ranges of the Courant and Peclet numbers. Possible options for minimizing numerical oscillations in the transport solutions include upstream weighing, artificial dispersion, and/or performance indexing.

### 3.2 Input data

The pore size distribution model of Mualem is used to predict the isothermal unsaturated hydraulic conductivity function from the saturated hydraulic conductivity as show in Eq. (1), the van Genuchten's model of the soil water retention curve is adopted as Eq. (2)<sup>12-13</sup>.

$$k = k_s \Theta^l [1 - (1 - \Theta^{\frac{1}{m_v}})^{m_v}]^2 \quad (1)$$

$$\Theta = \frac{1}{[1 + (-\alpha_v h)^{n_v}]^{m_v}} \quad (2)$$

Where  $k$  is unsaturated hydraulic conductivity,  $k_s$  is saturated hydraulic conductivity,  $\Theta$  is normalized water content,  $l$  is pore connectivity parameter,  $\alpha_v$ ,  $n_v$ ,  $m_v$  are fitting parameters.  $\alpha_v$  is related to the air entry value,  $n_v$  is related to the pore size distribution of the soil, it reflects the slope of soil water retention curve,  $m_v$  is related to the overall symmetry of the soil water retention curve. The thermal properties of sand soil implanted in HYDRUS-1D are recommended in this study. The hydraulic properties of K-7 sand are summarized in **Table 2**, which are inputs of numerical simulation.  $k_s$  was directly measured in laboratory. In addition, based on soil water retention curves that measured in the laboratory by using the Tempe Cell<sup>10</sup>, residual water content  $\theta_r$  and saturated water content  $\theta_s$  were determined, the parameters  $\alpha_v$ ,  $n_v$ , and  $l$  were assigned by optimally fitting soil water retention curves.

The upper boundary condition is the atmospheric boundary condition with surface layer, which consider no water runoff occurs during the tests. The lower boundary condition is the seepage face. Boundary conditions at soil surface for liquid water, water vapor, and heat transport were determined from the surface water and energy balance equations. The initial water contents and soil temperature are determined from measured values at the first day. The soil profile is considered to be 100 cm deep, with observation nodes locate at depths of 5 cm, 10 cm, 15 cm, 25 cm, 35 cm, 50 cm, 65 cm, 80 cm, and 95 cm. They are corresponded to the positions for thermocouples and soil water probe. A constant nodal spacing of 0.5 cm is used leading to 200 discretization nodes across the problem. Calculations are performed for a period of 81 days same with the monitored period.

**Table 2** Parameters used for the numerical simulation of field lysimeter test.

Soil	$\theta_r$ (cm <sup>3</sup> /cm <sup>3</sup> )	$\theta_s$ (cm <sup>3</sup> /cm <sup>3</sup> )	$\alpha_v$ (cm <sup>-1</sup> )	$n_v$ (dimensionless)	$k_s$ (cm/d)	$l$ (dimensionless)
K-7 sand	0.01	0.42	0.016	3.42	130	2.3

## 4. Result and Analysis

### 4.1 Field monitored data

Meteorological data were recorded from 27<sup>th</sup>, March to 15<sup>th</sup>, June of 2013, which are presented in **Fig. 3**. Six significant rainfall events that over 15 mm/d were recorded as marked in **Fig. 3(a)**. The precipitation in April and June were 3.78 mm/d and 4.50 mm/d respectively, higher than that mean value in May of 1.07 mm/d (**Fig. (b)**). The solar radiation was almost constant for these days at about 0.21 kW/m<sup>2</sup>. The air temperature varied between 3.4 °C and 30.7 °C, with a daily variation range at about 10 °C. **Figure 3 (c)** clearly shows that the average temperature has an increasing tendency during the period. The relative humidity in air varied between 30% and 90% (**Fig. 3 (d)**). It remained more or less constant until to the end of May, and then it went up day by day in June. The average wind speed was about 2.18 m/s, but several high speeds were recorded, for example, it reached 5.9 m/s and 5.5 m/s at 14<sup>th</sup> and 19<sup>th</sup> of April respectively.

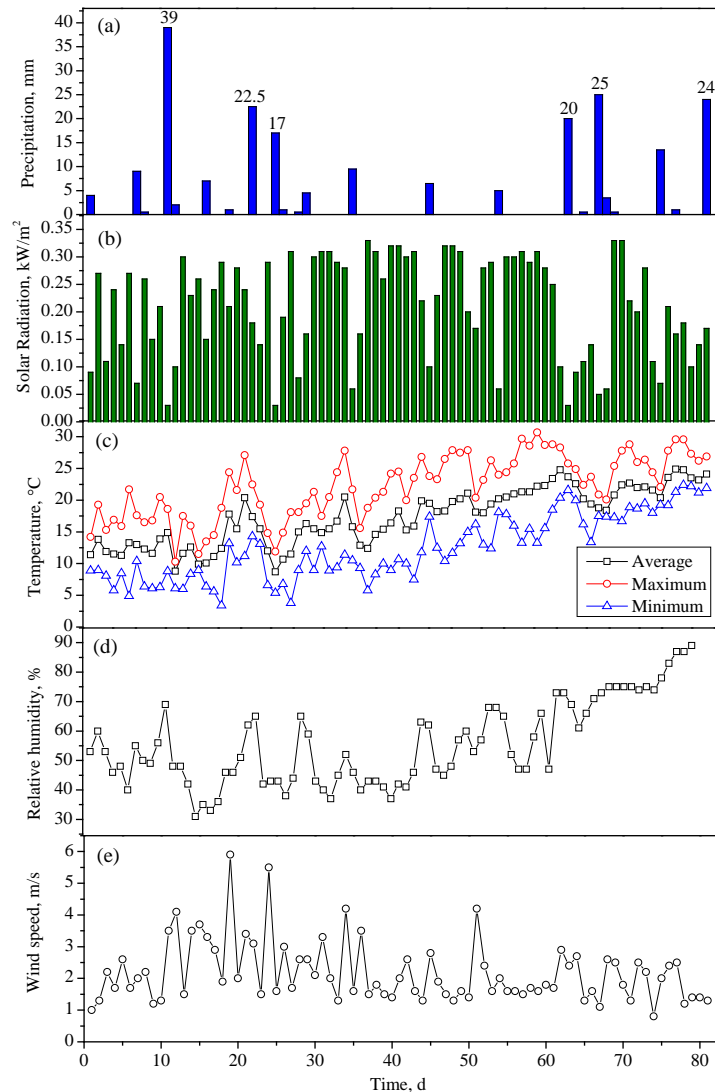


**Fig. 3** Meteorological data for 81 days that from Mar. 27, 2013 to Jun. 15, 2013, (a) precipitation, (b) solar radiation, (c) temperature, (d) relative humidity, and (e) wind speed.

**Figure 4** presents the variation of soil volumetric water content over the whole monitoring period at different depths. **Figure 4 (a)** shows that the soil at the top 25 cm was observed a sharp increase in water content corresponding to each rainfall event. The heavier precipitation resulted in greater increase of water content. And also the more near to the soil surface, the greater increase occurs. The soil at 5 cm produced 13% increase of volumetric water content in average, while they were 9%, 5% and 3% for the soil at 10 cm, 15 cm, and 25 cm respectively.

It presents a gradual decrease of volumetric water content at the top 25 cm after rainfall, it was due to the infiltration to the deeper layer and the evaporation to the atmosphere. A higher rate of water content decrease was observed for the soil at shallower position, which was mainly caused by the evaporation process since the infiltration can be regarded as same.

**Figure 4 (b)** shows that no significant change of water content at depths of 35 cm and 50 cm was observed expect for the heavy rainfall event, for example, the rain fall in April 6<sup>th</sup> resulted in about 5% and 2% increase of water content for 35 cm and 50 cm respectively. At other days, constant values of 24% and 26% were recorded for these two depths. Due to the experimental problem, the water content probe at 65 cm could not supply satisfied result. No significant changes occurred in the depths of 80 cm and 95 cm, where the soil stayed nearly saturation.

From the observations above, it seems that the a linear correlation between the precipitation/evaporation and volumetric water content changes at the top 25 cm, and the shallower the soil depth, the greater the value change. No significant influence was impacted for the precipitation/evaporation to the soil at deeper than 35 cm under the studied atmosphere condition.

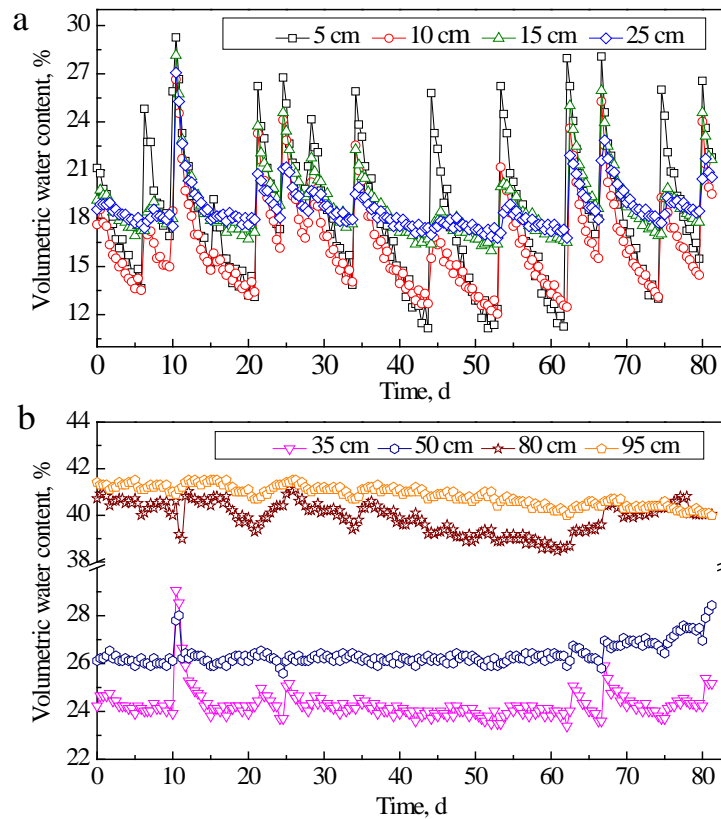


**Fig. 4** Variation of measured volumetric water content at different depths: (a) 5 cm ~ 25 cm, (b) 35 cm ~ 95 cm.

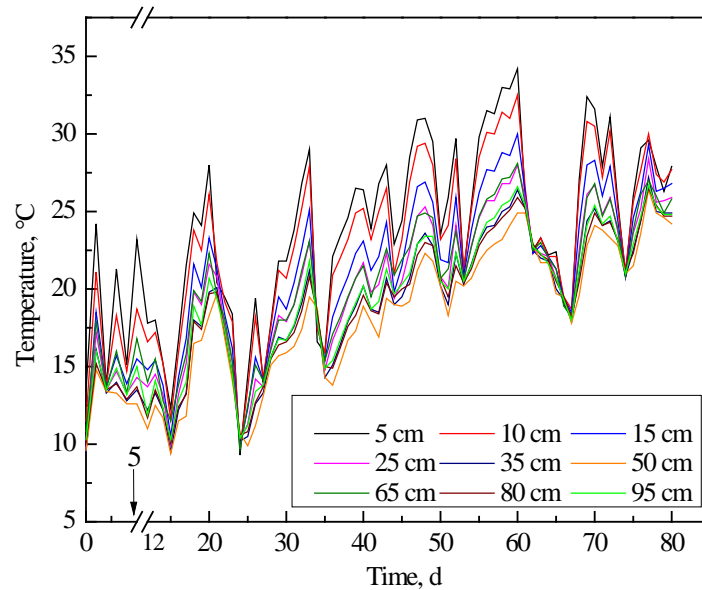


**Fig. 5** Monitored soil temperature variations at different depths during the test

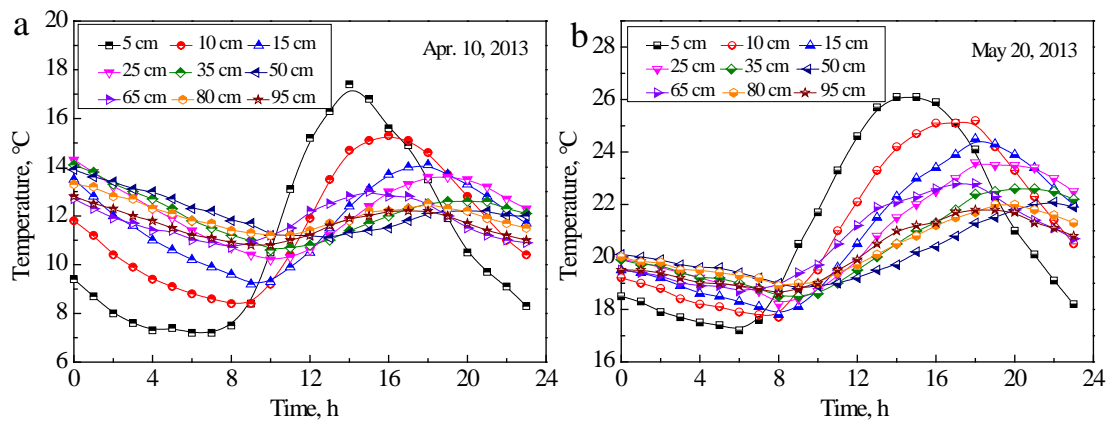


**Fig. 6** Monitored soil temperature variation in one day for the selected two days, (a) Apr. 10<sup>th</sup>, 2013 and (b) May 20<sup>th</sup>, 2013.

**Figure 5** presents the soil temperature measured at different depths during the test, where the daily temperature data at 14:00 pm are plotted against the elapsed time. Soil temperature was not recorded from 04:00 of April 2<sup>nd</sup> to 16:00 of April 8<sup>th</sup> due to experimental problems. It appears clearly that the shallower the soil depth, the greater the variation of soil temperature. The temperature at 50 cm seems to be the lowest value all the time, which may be due to the influence of external condition at shallower boundary. Comparing with the time for precipitation, it also shows that the water content decreases after rainfall, and the temperature gradient becomes non-significant, that means the rainfall produced the tendency to uniform soil temperature profile.

**Figure 6** shows the temperature variations of soil at different depths in 24 h for the selected two days, April 10<sup>th</sup> and May 20<sup>th</sup>. The soil temperature shows a typical sinusoidal behavior at all nine depths. The soil at surface maintains a greater range for temperature change from day to night. It produces a lowest temperature during night and a highest value at daytime. The amplitude of daily temperature variations decreased with depth due to attenuation of the transported heat energy. Also,



it is observed that the soil temperature increases gradually from top soil to the deeper one. Temperature difference of 5 °C between top and low boundary would be performed during daytime. The temperature gradient at the top 25 cm is several times greater than that of deeper soil.

#### 4.2 Variation of soil temperature and water content

**Figure 7** compares the simulated and measured soil temperature at three depths 5 cm, 50 cm, and 95 cm. The symbols represent the temperature measured at 14:00 pm of each day. On the whole, satisfactory agreement is obtained between the measured and calculated data. Nevertheless, the simulation for soil temperature at 5 cm only give a good trend of temperature variation, it is difficult to obtain accurate simulation over the whole monitoring period. For the soil temperature at 50 cm and 95 cm, the predicted soil temperature follow fairly well the measured values during the entire simulation period. However, in some period the simulated temperature amplitude is apart from the measured value. A greatest difference about 3 ~ 5 °C would be resulted in.

**Figure 8** shows the temperature profiles at different selected days. It can be observed that all the simulated temperature profiles fit well with the measured value, except for the profile at 5 days. From the simulation, temperature of top layer is lower than that of bottom soil; however, it is actually the inverse. This disagreement would be caused by the rainfall event at that day. It also indicates that the soil temperature changed at all the depths. The whole temperature profile increases from 5 days to 60 days, while the temperature profile at final condition shows a decreasing tendency, moreover, the temperature gradient along the depth is not obvious, thus it is deduced to be influenced by the rainfall.

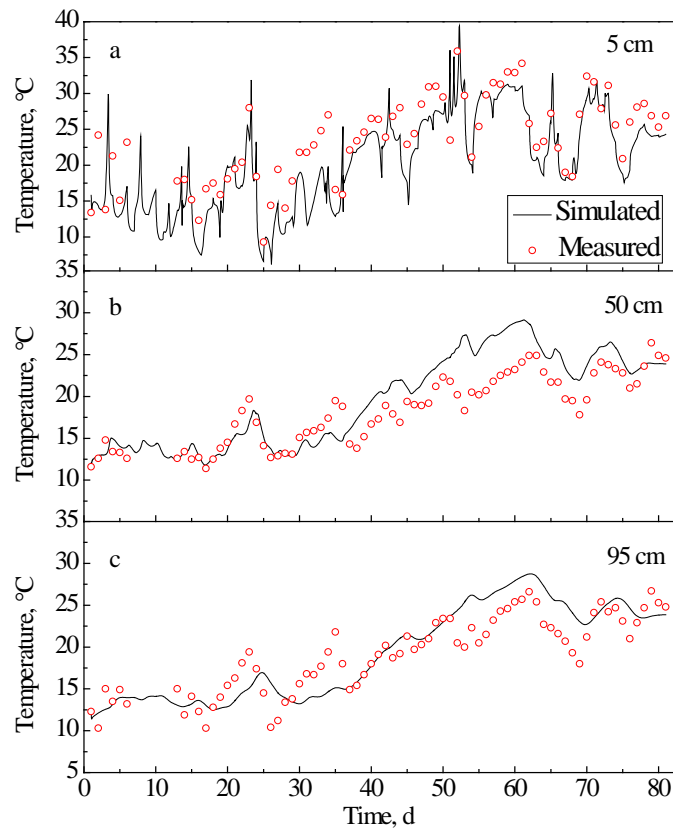


**Fig. 7** Comparison between numerical simulation and measurement for the soil temperature at three depths, (a) 5 cm, (b) 50 cm, and (c) 95 cm.

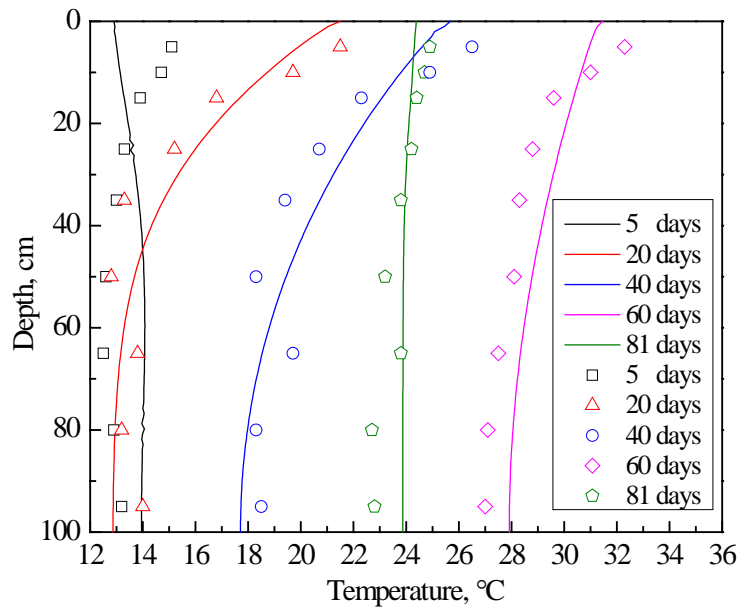


**Fig. 8** Comparison between simulated and measured soil temperature profile for the selected time, the solid lines represent numerical simulation result, symbols are the measured data.

**Figure 9** shows the comparison between simulated and measured volumetric water content at three selected depths: 5 cm, 15 cm, and 50 cm. Simulations are in rough agreement with measurements. For water content at 5 cm and 15 cm, some peaks and valleys at simulated curve is inconsistent with the measured value. For example, for the shape increase of water content at 12 days, the numerical simulation produces underestimation for both 5 cm and 15 cm. For the water content at 55 days, a significant overestimation is observed thereafter. In brief, rapid increases in water content at 5 cm and 15 cm depth after each rainfall are predicted reasonably well. The simulated and measured water content at 50 cm are almost constant during the simulation period while little difference exists between two curves.

**Figure 10** displays the simulated and measured water content profile at five different days. Good agreement can be observed between the solid lines and symbols. A small difference between symbols and lines can be appreciated. It shows that the volumetric water content increase linearly with the soil depth, a linear correction can be obtained except the profile at 81 days. Due to the influence of rainfall, the water content profile changes at the 81 days, the water content of top 40 cm increases significantly. Moreover, it indicates that the deeper the water content, the smaller gradient of the water content. That is because the soil at deeper layer maintain at a condition nearly saturated, the rainfall and evaporation cycle has little influence.

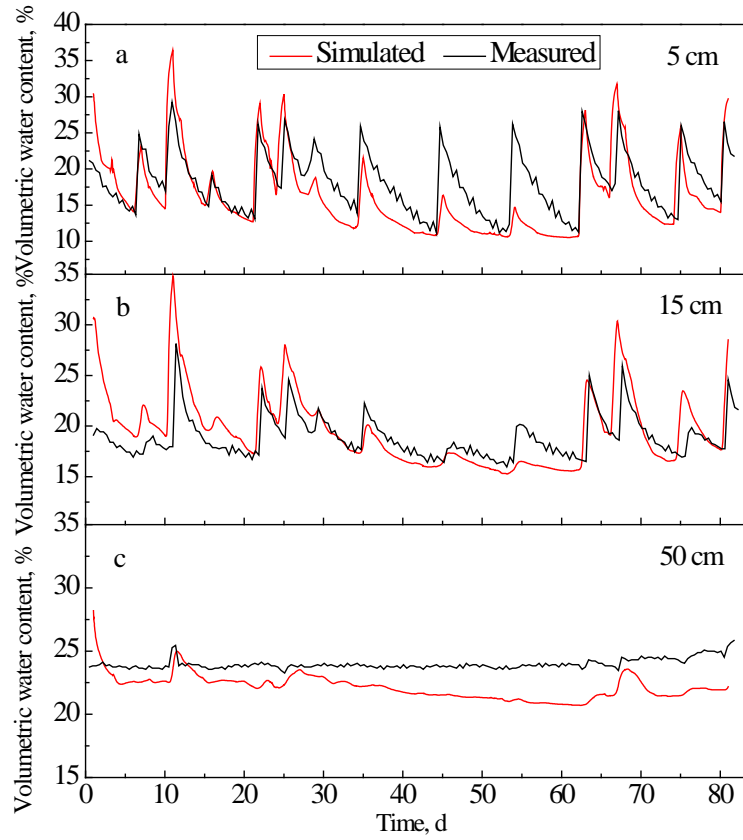


**Fig. 9** Comparison between simulated and measured water content at three different depths, (a) 5 cm, (b) 15 cm, and (c) 50 cm.

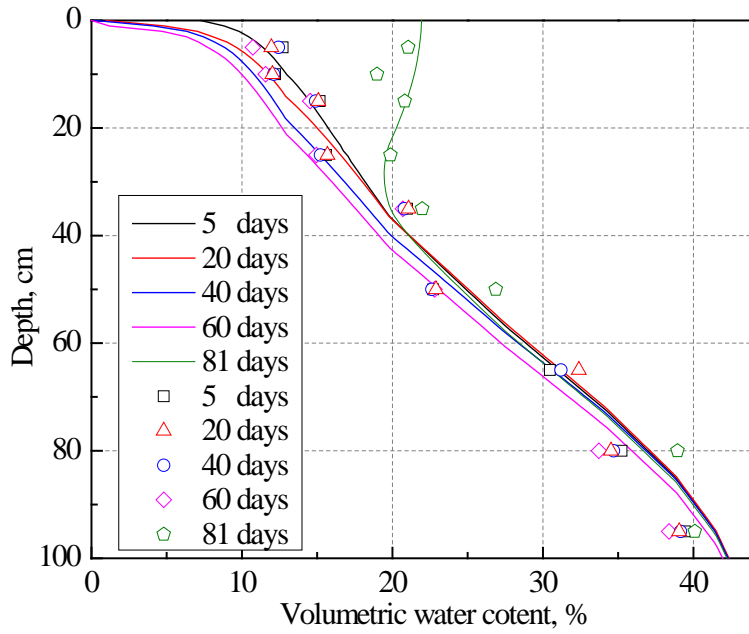


**Fig. 10** Comparison between simulated and measured water content profile

### 4.3 Drainage and evaporation

**Figure 11** presents the comparison between the calculated and the measured cumulative water drainage from the bottom. The solid line follows fairly well the tendency of measured cumulative drainage. There is a little difference between the total amount of water flowed out, the measured value is about 12.2 cm during 81 days, while the simulated result is around 11.6 cm. The greatest difference appears at about the 65 days, where the disagreement is large to 3.5 cm. In addition, in the first 10 days, a gap between the measured and simulated value is observed, the difference is around 2.5 cm, the percolation would occur due to the high water content profile that is the initial condition of numerical simulation, however, no water flowed out in actual testing condition. It shows that the percolation always occurs after each rainfall event. For the heavy rainfall event, about 2 days are consumed for the soil water flowing out and achieving an equilibrium state. At that time, amount of water drainage is close to rainfall amount, because the soil body is nearly saturated with no more water can be retained, the soil can be considered as a media for water migration from top to bottom.

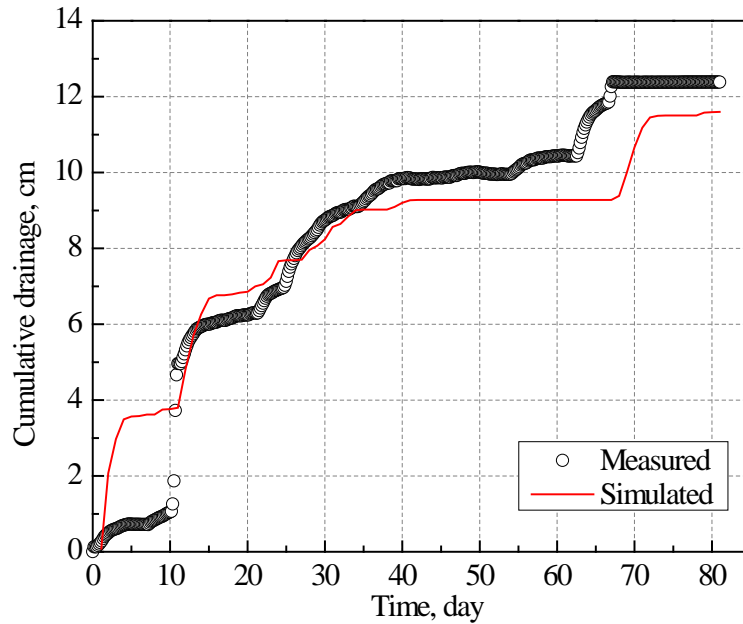


**Fig. 11** Variation of cumulative drainage: comparison between simulation and measurement.

The evaporation rate can also be determined from lysimeter test by considering the conservation of mass of water into and out of the lysimeter, the evaporation may be obtained as follows:

$$E = P - G_p - \Delta S - R_{off} \quad (3)$$

where  $E$  is evaporation,  $P$  is precipitation,  $G_p$  is basal percolation,  $\Delta S$  is changes in moisture storage,  $R_{off}$  is surface water runoff. The rainfall can be measured from the weather station and no runoff is assumed during the test, that is to say, all the precipitation is infiltrated into the soil. The percolation is channeled from the lysimeter by weight and measured in a drainage tank, the water storage is estimated from the water content profile that measured by the water moisture probe. The lysimeter in this study as a kind of weighting lysimeter, allows direct measurement of evaporation since it can measure the total weight of soil and stored water. Changes of soil water storage in a

lysimeter can be determined by integrating profiles of water content. Consequently, the remaining changes in mass can be attributed to losses by evaporation.

The comparison between simulated and measured cumulative evaporation is displayed in **Fig. 12**. The simulated cumulative evaporation increases linearly with the elapsing time. It shows that the cumulative evaporation increases with pause for each rainfall event. The total amount of water evaporated loss is about 10 cm, equals to 1.25 mm/d in average during the in-situ test. The symbols are dispersed each other, which due to the error when integrating profiles of water content, deviation of total weight caused by the sensitivity of load cell is also attribute to this error. Although the measured volumetric water content is discrete, it clearly shows the linear correlation and is agreed well by the simulated result. A conclusion remark is that a significant error would be resulted in using the weighting lysimeter, an optimal design are conducted with both considering the test section and capacity of scales.

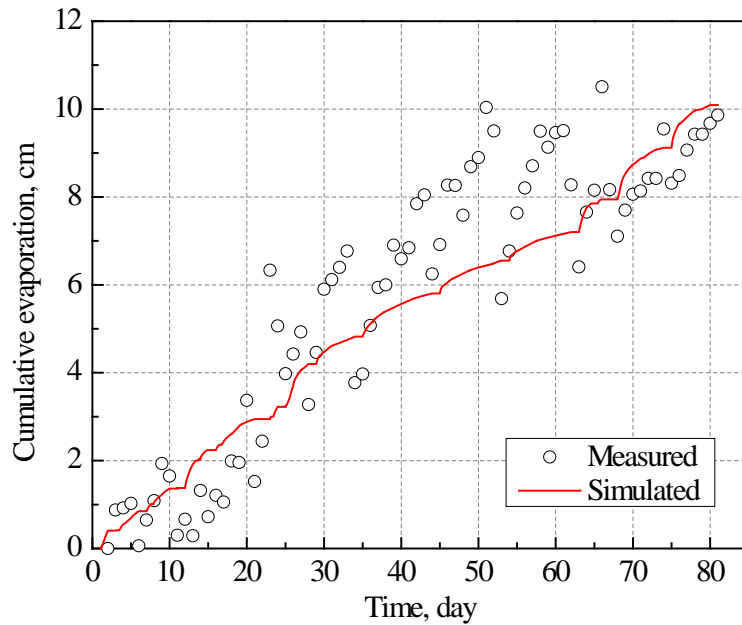


**Fig. 12** Variation of cumulative evaporation from soil surface: comparison between simulation and measurement.

## 5. Conclusions

In this paper, an in-situ test conducted in Ito campus of Kyushu University from 27<sup>th</sup>, March to 15<sup>th</sup>, June of 2013 is presented, it provides an extensive database of environmental parameters and the reaction of sandy soil properties. The thermal and hydrological phenomena caused by atmosphere change are analyzed in this study. These data is also used to compare with the numerical simulation based on HYDRUS-1D code. The conclusions can be summarized as following:

- (1) The volumetric water content in the near surface-zone is strongly affected by the precipitation and evaporation processes. The most significant range is limited at the top 35 cm. The volumetric water content exhibits a nearly linear relationship with the depth. Moreover, the shallower the soil depth, the greater the change in water content responding to evaporation or precipitation.

- (2) Soil temperature increases gradually from top soil to the deeper one with temperature gradient of about 0.05 °C/cm. Soil temperature varied for all depths, which suggests that soil temperature is more sensitive to climate change than water content.
- (3) The rainfall event shows the function of eliminating temperature and water content gradient in soil, while the evaporation process enlarges the gradient of temperature and water content. The recorded date also provides the evidence that the temperature of rainfall water directly affects the soil temperature, which was often neglected in previous research.
- (4) Field measurement evaluates the relevance of the numerical model, it is found that the numerical approach adopted in this paper can provide a reasonable predication for the variation of temperature and water content.

The recorded date allow the mechanism of soil-atmosphere interaction to be revealed, they can be also used to verify existing models for soil water evaporation or to develop new ones. From a practical point of view, although the adopted code provides a relatively direct countermeasure, a two-dimensional or three dimensional model is essential for a full geometry analysis, an analytical model as an easily preformed approach is also highly required to reveal the in-situ mechanism of soil-atmosphere.

### **Acknowledgements**

This research is supported by Grant-in Aid for scientific research (A) No.22246064 (Project leader: Prof. Noriyuki Yasufuku), from Japan Society for the Promotion of Science (JSPS). The authors acknowledge the supports. The authors are pleased to Professor Hemant Hazarika, Assistant Professor Ryohei Ishikura, and Dr. Qiang Liu for their astonishing advice. In addition, it is indebted to Laboratory Assistant Mr Michio Nakashima who has made available continuous shore up in a number of ways.

### **References**

- 1) H. Saito, J. Šimunek, and B.P. Mohanty; Numerical analysis of coupled water, vapor, and heat transport in the vadose zone, *Vadose Zone Journal*, Vol.5, pp.784-800 (2006).
- 2) G.W. Wilson, D.G. Fredlund, S.L. Barbour; Coupled soil-atmosphere modeling for soil evaporation, *Canadian Geotechnical Journal*, Vol.31, pp.151-161 (1994).
- 3) E.K. Yanful, S.M. Mousavi, M. Yang; Modeling and measurement of evaporation in moisture-retaining soil covers, *Advances in Environmental Research* Vol.7, pp.783-801 (2003).
- 4) J.W. Gowing, F. Konukcu, D.A. Rose; Evaporative flux from a shallow water table: The influence of a vapour-liquid phase transition, *Journal of Hydrology*, Vol.321, pp.77-89 (2006).
- 5) J.D. Teng, Y. Noriyuki, Q. Liu, S.Y. Liu; Analytical solution for soil water redistribution during evaporation process, *Water Science and Technology*, Vol.68, No.12, pp.2545-2551 (2013).
- 6) Y.J. Cui, Y.F. Lu, P. Delage, M. Riffard; Field simulation of in situ water content and temperature change due to ground-atmosphere interactions, *Géotechnique*, Vol.55, No.7, pp.557-567 (2005).
- 7) P. Rajeev, D. Chan, J. Kodikara; Ground-atmosphere interaction modelling for long-term prediction of soil moisture and temperature, *Canadian Geotechnical Journal*, Vol.49, pp.1059-1073 (2012).
- 8) J.D. Teng; Evaluation of soil-atmosphere interaction during evaporation process, Ph.D. dissertation, Kyushu University, Fukuoka (2013).
- 9) J.O. Payero, and S. Irmak; Construction, installation, and performance of two repacked

weighing lysimeters, *Irrigation Science*, Vol.26, pp.191-202 (2008).

- 10) J. Šimunek, M.Th. van Genuchten, and M. Šejna; The HYDRUS-1D software package for simulating the. One-dimensional movement of water, heat, and multiple solutes in variably-saturated media, Version 3.0. HYDRUS Software Series 1, Department of Environmental Sciences, University of California Riverside, Riverside, California, USA, (2005).
- 11) Q. Liu; Development and evaluation of self-watering system in unsaturated arid ground, Ph.D. dissertation, Kyushu University, Fukuoka (2010).
- 12) Y. Mualem; A new model for predicting the hydraulic conductivity of unsaturated porous media, *Water Resource Research* Vol.12, pp.513-521 (1976).
- 13) M.Th. van Genuchten; A closed form equation for predicting the hydraulic conductivity of unsaturated soils, *Soil Science Society of America Journal*, Vol.44, pp.892-898 (1980).